

Conformation of Sequential Polypeptide Containing Z-Dehydrophenylalanine Residues

Yoshihito INAI,* Takaaki ITO, Tadamichi HIRABAYASHI,
and Kenji YOKOTA

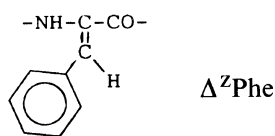
Department of Materials Science and Engineering, Nagoya Institute of Technology,
Gokiso-cho, Showa-ku, Nagoya 466, Japan

(Received February 9, 1995)

ABSTRACT: A sequential polypeptide containing Z-dehydrophenylalanine (Δ^Z Phe) residues, poly[Lys(Z)- Δ^Z Phe-Aib], was synthesized to realize a highly stable helical backbone for regularly arranging the β -substituents of dehydroresidues. The polypeptide was prepared by polymerizing the corresponding tripeptide with diphenylphosphoryl azide and fractionated into different molecular weight (MW) species. The polypeptides showed CD profiles with exciton couplets around 276 nm in chloroform, in trimethyl phosphate, and in trifluoroacetic acid, indicating that β -phenyl groups are arranged regularly along the right-handed helical backbone having high conformational stability. Average main-chain conformations in solution of a series of peptides (X- Δ^Z Phe-Aib)_n ($n=2, 3, 4$, and >4) were estimated by considering conformational energies, and experimental and theoretical CD amplitudes at the same time. Oligopeptides Boc-(Ala- Δ^Z Phe-Aib)_n-OMe ($n=2-4$) were shown to form a right-handed 3_{10} -type helix that contains 3.2–3.3 residues per turn. The polypeptide also formed a right-handed helix but, with increasing MWs, this helix deviated from that of oligopeptides and showed a tendency to form an α -type helix.

KEY WORDS Z-Dehydrophenylalanine / Sequential Polypeptide / CD
Study / Helical Conformation /

α,β -Dehydroamino acid residues are present naturally in many peptides having biological activity and in some proteins.^{1–5} These residues in (poly)peptides have been found to influence main-chain conformations due to the presence of $C^\alpha=C^\beta$ double bonds having inherent structural features: *i.e.*, planarity around the $C^\alpha=C^\beta$ and trigonal geometry of C^α . For Z- α,β -dehydrophenylalanine (Δ^Z Phe), this residue favors the formation of β -turn structures in small peptides.⁶



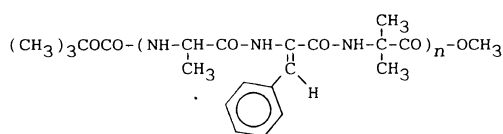
Recently, linear oligopeptides containing two or three Δ^Z Phe residues have been found in helical structures.^{7–14} Thus, Δ^Z Phe is an im-

portant element for optimally-designing not only β -turn, but also helical backbones.

Also, the Δ^Z Phe residue is expected to have a specific conformational space for its side chain. In particular, side-chain freedom will be smaller than those for naturally occurring amino acids such as Phe, Glu, and Lys,^{15–17} because of prohibited rotation about $C^\alpha=C^\beta$ double bonds. Thus, such β -substituted α,β -dehydroalanines attract much interest as unique residues to provide a rigid and regular molecular frame for arranging β -substituents along a peptide backbone.

To demonstrate the rigidity of the molecular frame of β -substituted α,β -dehydroalanines, we synthesized sequential oligopeptides containing helicogenic Δ^Z Phe and α -aminoisobutyric acid (Aib) residues⁶:

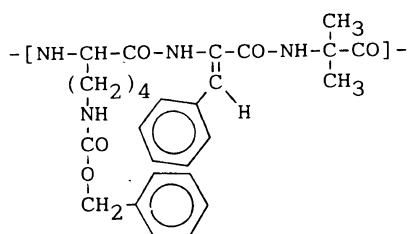
* To whom correspondence should be addressed.



Boc-(Ala- Δ^Z Phe-Aib) $_n$ -OMe $n=2-4$: **I-n**¹⁸
(Boc, *t*-butoxycarbonyl; OMe, methoxy)

The peptides **I-n** formed a right-handed helix, which has the 3_{10} -helical-type [$i \leftarrow (i+3)$] H-bonding pattern, and the Δ^Z Phe side chains are arranged regularly along the helix.

To extend this study, we used the corresponding sequential polypeptide:



poly[Lys(Z)- Δ^Z Phe-Aib] **II**
[Lys(Z), N^ϵ -[(benzyloxy)carbonyl]-L-lysine]

Little is known about the synthesis and conformational analysis of sequential polypeptides containing Δ^Z Phe residues. Our purpose is to design and synthesize a polypeptide having helically- and regularly-arranged Δ^Z Phe side chains, and investigate its conformation. The conformation was estimated by CD measurement, and theoretical CD and conformational energy calculations. The conformation of peptides **I-n** was reexamined by the same methods. On the basis of these results, the solution conformation of the sequential polypeptides is discussed.

EXPERIMENTAL

Materials

Polypeptide **II** was prepared by polymerizing the corresponding tripeptide, H-Lys(Z)- Δ^Z Phe-Aib-OH, with diphenylphosphoryl azide (DPPA).¹⁹ The *N*-protected peptide, Boc-

Lys(Z)- Δ^Z Phe-Aib-OH **III**, was synthesized by a similar manner for the preparation of Boc-Ala- Δ^Z Phe-Aib-OH.¹⁸ All intermediates including peptide **III** were checked for purity by ¹H NMR and IR spectroscopy, thin-layer chromatography (TLC), and gel permeation chromatography (GPC). Solvent systems for TLC were (A) ethyl acetate, (B) chloroform-methanol (9:1), and (C) *n*-butanol-acetic acid-water (4:1:1). GPC was recorded on a Tosoh HLC-803-D equipped with G1000-, G2500-, and G3000-HXL columns in series, using tetrahydrofuran eluent. Single spots in the TLC and single peak in the GPC were obtained. The molecular weight (MW), number-averaged MW (M_n), and weight-averaged MW (M_w) for polypeptide were estimated by GPC with reference to polystyrene standards. mp, TLC, GPC, and spectral data for peptide **III** and other intermediates were as follows.

Boc-Lys(Z)- Δ^Z Phe Azlactone: mp 134–135°C; $R_f^A=0.85$; $R_f^B=0.75$; $R_f^C=0.96$; GPC retention time=23.4 min. ¹H NMR (δ , ppm from tetramethylsilane (TMS) in CDCl₃): 7.4–8.2 (5H, m, aromatic protons Δ^Z Phe), 7.3 (5H, s, aromatic protons Lys(Z)), 7.2 (1H, s, C ^{β} H Δ^Z Phe), 5.1 (2H, s, benzyl protons Lys(Z)), 5.1 (1H, br, NHC ^{α} Lys(Z)), 4.7 (2H, m, NHC ^{ϵ} and C ^{α} H Lys(Z)), 3.2 (2H, m, C ^{ϵ} H₂ Lys(Z)), 1.3–2.0 (6H, m, (CH₂)₃C ^{α} Lys(Z)), and 1.5 (9H, s, 3 × CH₃ Boc). IR (cm⁻¹, NaCl): 3350 (NH), 1790 (C=O), 1680 (C=O), 1600 (C=N), and 1520 (NH).

Boc-Lys(Z)- Δ^Z Phe-Aib-OMe: mp 157–161°C; $R_f^A=0.70$; $R_f^B=0.73$; $R_f^C=1.0$; GPC retention time=23.2 min. ¹H NMR (δ , ppm from TMS in CDCl₃): 7.5 (1H, s, NH Δ^Z Phe), 7.2–7.5 (11H, m, aromatic protons, and C ^{β} H Δ^Z Phe), 7.2 (1H, s, NH Aib), 5.3 (1H, br, NHC ^{α} Lys(Z)), 5.1 (2H, s, benzyl protons Lys(Z)), 5.0 (1H, br, NHC ^{ϵ} Lys(Z)), 4.1 (1H, m, C ^{α} H Lys(Z)), 3.7 (3H, s, methoxyl protons), 3.2 (2H, m, C ^{ϵ} H₂ Lys(Z)), 1.3–2.0 (6H, m, (CH₂)₃C ^{α} Lys(Z)), 1.6 (6H, d, 2 × CH₃ Aib), and 1.5 (9H, s, 3 × CH₃ Boc). IR (cm⁻¹, NaCl): 3320 (NH), 1680 (C=O), and 1520 (NH).

Boc-Lys(Z)- Δ^2 Phe-Aib-OH: gradually decomposed at 88–105°C; $Rf^A = 0-0.11$; $Rf^B = 0.35$; $Rf^C = 0.89$; GPC retention time = 23.0 min; $^1\text{H NMR}$ (δ , ppm from TMS in CDCl_3): 8.2 (1H, br, NH Δ^2 Phe), 7.4 (1H, br, NH Aib), 7.2–7.5 (11H, m, aromatic protons and C^βH Δ^2 Phe), 4.8–5.4 (3H, br, $2 \times \text{NH Lys(Z)}$ and COOH), 5.1 (2H, s, benzyl protons Lys(Z)), 4.2 (1H, m, $\text{C}^\alpha\text{H Lys(Z)}$), 3.2 (2H, m, $\text{C}^\epsilon\text{H}_2$ Lys(Z)), 1.6–2.0 (6H, m, $(\text{CH}_2)_3\text{C}^\alpha$ Lys(Z)), 1.6 (6H, s, $2 \times \text{CH}_3$ Aib), and 1.4 (9H, s, $3 \times \text{CH}_3$ Boc). IR (cm^{-1} , NaCl): 3300 (NH and OH), 1690 (C=O), and 1520 (NH).

Polymerization

Boc-Lys(Z)- Δ^2 Phe-Aib-OH was dissolved in formic acid and allowed to stand for 5 h at room temperature. The formic acid was evaporated *in vacuo* and the residue was dissolved in 5% NaHCO_3 aqueous solution. Solution pH was adjusted to *ca.* 6 with 5% KHSO_4 aqueous solution, and the white precipitate was collected and dried *in vacuo*.

To a mixture of the above H-Lys(Z)- Δ^2 Phe-Aib-OH (92 mg, 0.18 mmol) and dimethyl sulfoxide (0.1 mL) were added DPPA (42 μL , 0.2 mmol) and *N*-methylmorpholine (24 μL , 0.2 mmol) at 5–10°C. The mixture was stirred vigorously at 5–10°C for 2 h, and stirring was continued for 48 h at room temperature. To the mixture was added a large volume of water, and the precipitate was collected by centrifugation. The precipitate was washed with water and then methanol, and dried *in vacuo*. The obtained polypeptide was fractionated into three species of low (II-L), middle (II-M), and high (II-H) MWs by chromatography on a column of Sephadex LH-60/*N,N*-dimethylformamide. Their M_n /polydispersity indices (M_w/M_n)/yields were $5.2 \times 10^3/1.6/9$ mg for II-L, $9.0 \times 10^3/2.2/9$ mg for II-M, and $2.0 \times 10^4/2.4/2.4$ mg for II-H. The three $^1\text{H NMR}$ spectra in CDCl_3 were almost the same: δ (ppm from TMS), 9.5 (1H, br, NH Δ^2 Phe); 7.8–8.2 (2H, br, NH Aib and NH Lys(Z)); 6.5–7.6 (11H, br, aromatic protons and C^βH Δ^2 Phe); 5.4 (1H,

br, NHC^ϵ Lys(Z)); 5.0 (2H, br, benzyl protons Lys(Z)); 4.2 (1H, br, $\text{C}^\alpha\text{H Lys(Z)}$); 3.2 (2H, br, $\text{C}^\epsilon\text{H}_2$ Lys(Z)); 1.0–2.2 (12H, br, $(\text{CH}_2)_3\text{C}^\alpha$ Lys(Z) and $2 \times \text{CH}_3$ Aib).

Measurements

$^1\text{H NMR}$ spectra were recorded using a Varian XL-200 spectrometer (200 MHz) and Hitachi R-90 spectrometer (90 MHz). Measurements were carried out with a CDCl_3 solution of 5–20 mg ml^{-1} . CD and UV spectra were simultaneously recorded using a JASCO J-600. The measurements were carried out with a chloroform, trimethyl phosphate (TMP), or chloroform/trifluoroacetic acid (TFA) solution of $[\Delta^2\text{Phe}] = 3 \times 10^{-5}$ M. The concentration of the $\Delta^2\text{Phe}$ residue was determined by maximum absorbance around 275 nm. The molar extinction coefficient per $\Delta^2\text{Phe}$ residue for I-4 ($\epsilon_{274} = 1.8 \times 10^4$) was used.¹⁸ Chloroform, TMP, and TFA were purified by distillation before use.

Energy and Theoretical CD Calculations

Empirical conformational energy calculations were carried out using structural and energy parameters based on ECEPP system.²⁰ The parameters for $\Delta^2\text{Phe}$ residue were determined in the previous study.¹⁸ The two-fold rotational barriers in a $\Delta^2\text{Phe}$ residue were taken to be 10 kcal mol^{-1} for the ϕ angle, 8 kcal mol^{-1} for the ψ ,^{21–23} and 6.4 kcal mol^{-1} for the χ_2 .²³ The program PEPCON, written by Sisido²⁴ for conformational energy calculation and graphics²⁵ of a given peptide, was modified to be applicable to $\Delta^2\text{Phe}$ -containing peptides. By this program, the main-chain energy contour map for a $\Delta^2\text{Phe}$ residue was calculated. This map essentially resembled that reported by Ajo *et al.*,^{6,23,26} whose map reflects experimental structural data of $\Delta^2\text{Phe}$ -containing peptides well.⁶

Conformational energy of polypeptide II was calculated for $\text{Ac}(\text{Ala}-\Delta^2\text{Phe}-\text{Aib})_8\text{-NMA}$ (Ac, acetyl; NMA, *N*-methylamide), where Ala was used instead of Lys(Z) to

simplify calculation.²⁷⁻²⁹ Based on many crystallographic data of Δ^Z Phe-containing peptides,^{6-11,13} all amide groups were fixed to the *trans* conformation ($\omega=180^\circ$) and each Δ^Z Phe side-chain (χ_1) was fixed to 0° . Two methods were used to predict the conformation of polypeptide **II**. One is to calculate the main-chain energy contour map by changing all ϕ and ψ at 5° (or at 1° for expanded contour map). In each (ϕ, ψ) , the χ_2 angle in Δ^Z Phe residue was taken as the value that gives the minimal conformational energy. The other, developed by Oka,^{30,31} is to search all possible helical conformations by stepwise expansion of the sequential peptides $(\text{Ala}-\Delta^Z\text{Phe}-\text{Aib})_n$. In the first step, energy minimization for the tripeptide, $\text{Ac}-\text{Ala}-\Delta^Z\text{Phe}-\text{Aib}-\text{NMA}$, was carried out. Here all combinations of energy minima of Ala, Δ^Z Phe, and Aib residues ($5 \times 20 \times 7$) were used as starting conformations. The second step was minimization for the hexapeptide having two repeating units of $\text{Ala}-\Delta^Z\text{Phe}-\text{Aib}$, *i.e.*, $\text{Ac}-(\text{Ala}-\Delta^Z\text{Phe}-\text{Aib})_2-\text{NMA}$. Here all minima in the first step were used as starting conformations of the second step. Also, the third step was the minimization of $\text{Ac}-(\text{Ala}-\Delta^Z\text{Phe}-\text{Aib})_4-\text{NMA}$ using all minima in the second step as starting conformations of the third step. Finally, the minimization of $\text{Ac}-(\text{Ala}-\Delta^Z\text{Phe}-\text{Aib})_8-\text{NMA}$ was carried out using all minima in the third step. All minimizations were carried out for six variables, ϕ_{Ala} , ψ_{Ala} , $\phi_{\Delta^Z\text{Phe}}$, $\psi_{\Delta^Z\text{Phe}}$, $\chi_{2,\Delta^Z\text{Phe}}$, ϕ_{Aib} , and ψ_{Aib} , using the Simplex algorithm. The conformations were also expressed by the conformational letter code that divides 16 regions in conformational space.³²

Theoretical CD spectra were calculated by the exciton chirality method.³³ Only the low energy $\pi-\pi^*$ transition around 276 nm of Δ^Z Phe residue was considered. The detailed calculation procedure is described in the previous study.¹⁸

RESULTS AND DISCUSSION

CD Studies

UV absorption spectra of the polypeptides showed an intense band around 276 nm (data not shown), referred as "band I" previously¹⁸ and assigned to a Δ^Z Phe transition. The band gave essentially the same profile as observed for oligopeptides **I-2** to **I-4**. This indicates that the transition properties of Δ^Z Phe residue do not change for the polypeptides and oligopeptides.

Figure 1 shows the corresponding CD spectra of polypeptides **II-H**, **II-M**, and **II-L** as well as peptides **I-2** to **I-4** recorded in chloroform. The molar ellipticity in the ordinate is expressed with respect to the concentration of Δ^Z Phe residue. Peptides **I-2** to **I-4** showed strong exciton couplets with a negative peak at longer wavelengths. These couplets have already indicated that peptides **I-2** to **I-4** form a right-handed helix that has 3_{10} -helical type H-bonding pattern and contains more than three residues per turn.¹⁸

Polypeptides **II-H**, **II-M**, and **II-L** showed exciton couplets with the same sign as that of peptide **I-4**. Obviously, the transition moments of band I in the polypeptides are arranged in

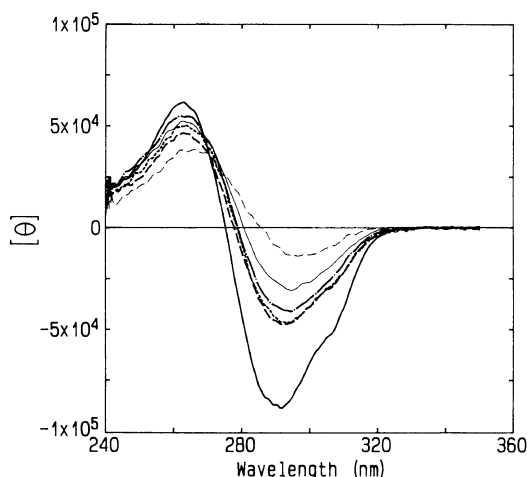


Figure 1. CD spectra of **II-H** (—), **II-M** (-----), **II-L** (·····), **I-4** (— · —), **I-3** (—), and **I-2** (-----) in chloroform.

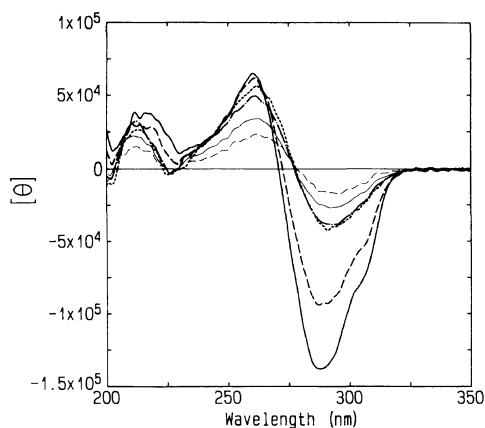


Figure 2. CD spectra of **II-H** (—), **II-M** (-----), **II-L** (·····), **I-4** (— · —), **I-3** (—), and **I-2** (-----) in TMP.

a similar manner to peptide **I-4**, *i.e.*, along a right-handed helical main chain. These helical conformations for the polypeptides were also supported by ^1H NMR data in CDCl_3 : their $\Delta^Z\text{PheNH}$ and AibNH resonances appeared at *ca.* 9.5 ppm and at *ca.* 8.0 ppm, respectively. These positions correspond to those of intramolecularly H-bonding NH resonances in peptides **I-2** to **I-4** with a helical structure in CDCl_3 .¹⁸

The amplitude of exciton couplet for polypeptide **II-H** with the longest chain lengths was markedly larger than those for the other polypeptides and peptide **I-4**. Amplitude increase with chain length was also observed in TMP more prominently (Figure 2): amplitudes were 8.8×10^4 for peptide **I-4**, 9.8×10^4 for **II-L**, 16×10^4 for **II-M**, and 20×10^4 for **II-H**.

This chain-length dependence on CD amplitudes might be interpreted as follows. First, the increase of chain lengths enhances the structural stability of peptides $(\text{X}-\Delta^Z\text{Phe-Aib})_n$, because CD amplitudes, in general, tend to increase with decreasing irregularity and thermal fluctuations in a specific conformation. Secondly, conformational changes, *e.g.*, helix interconversion, are induced by variation of chain lengths. Theoretical amplitudes (A_1) estimated by theoretical CD calculation are

sensitive to the spatial arrangements of $\Delta^Z\text{Phe}$ chromophores along a helix.¹⁸ In particular, A_1 increases with screw angle (τ) between $\text{C}^\alpha = \text{C}^\beta$ vectors of the nearest $\Delta^Z\text{Phe}$ pair(s), *e.g.*, on changing from 3_{10} -helical (three residues per turn, *i.e.*, $\tau = 0^\circ$) to α -helical (3.6 residues per turn, *i.e.*, $\tau = 60^\circ$) main chains.

Helical Stability

Relative helical stabilities for polypeptides are discussed from the effect of adding a helix-destabilizing solvent (TFA) on their CD spectra. Figures 3(a) and 3(b) show CD spectra of polypeptides **II-L** and **II-H** in chloroform/TFA mixtures with varying TFA content. With TFA content increasing, the CD patterns for both polypeptides shifted to longer wavelengths gradually. This red shift is responsible for the red shift of the corresponding absorption band I. The shift of the band I may be induced by high polarity or strong H-bond donating nature of TFA, because this band is assigned to an intramolecular charge-transfer interaction between styryl and carbonyl groups in the $\Delta^Z\text{Phe}$ residue.³⁴ However, the transition properties in the presence of TFA should be similar to those in the absence of TFA, because the absorption profile did not change essentially in the absence of and presence of TFA. Accordingly, the change of CD spectra with adding TFA can be ascribed to qualitative conformational change induced by TFA.

The exciton couplets observed for polypeptides **II-L** and **II-H** in chloroform were retained in chloroform/TFA mixtures, and interestingly in 100% TFA. Namely, helical structures of the polypeptides remain to some degree even in 100% TFA. Solvent-induced conformational transitions were reported for poly(L-1- and L-2-naphthylalanine)s.³⁰ The two polypeptides had a helical conformation in 1,2-dichloroethane, but at TFA content of 3–5 vol% or more, poly(L-1-naphthylalanine) changed to an extended β -structure and poly(L-2-naphthylalanine) did to a randomly coiled conformation. Therefore, poly[Lys(Z)-

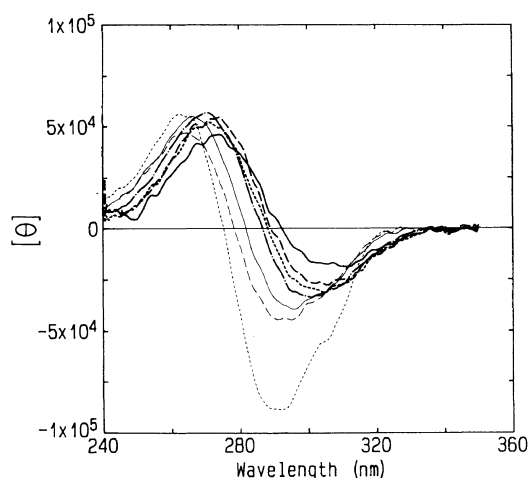


Figure 3(a). CD spectra of **II-H** in chloroform/TFA mixed solvents. TFA content (v/v %): 0 (·····), 0.5 (-----), 1 (—), 5 (— · —), 20 (·····), 50 (-----), and 100 (—).

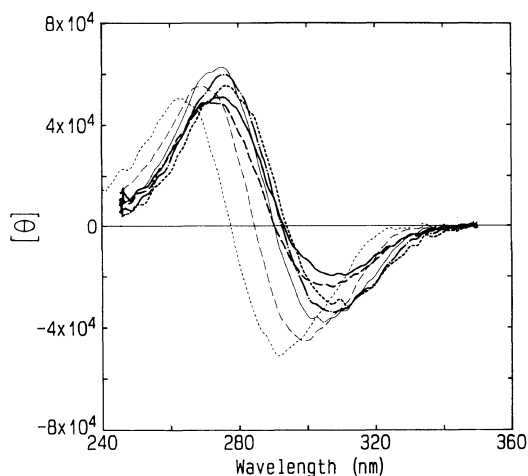


Figure 3(b). CD spectra of **II-L** in chloroform/TFA mixed solvents. TFA content (v/v %): 0 (·····), 0.5 (-----), 2 (—), 5 (— · —), 20 (·····), 50 (-----), and 100 (—).

Δ^Z Phe-Aib] forms a much more stable helix than poly(naphthylalanine)s that consist of saturated amino acids.

The amplitudes of exciton couplets for polypeptides **II-L** and **II-H** decreased with increasing TFA content. Figure 4 plots minimal $[\theta]$ in exciton couplets ($[\theta]_{\min}$) against TFA content. For polypeptide **II-L**, $[\theta]_{\min}$ increased moderately with TFA content. For

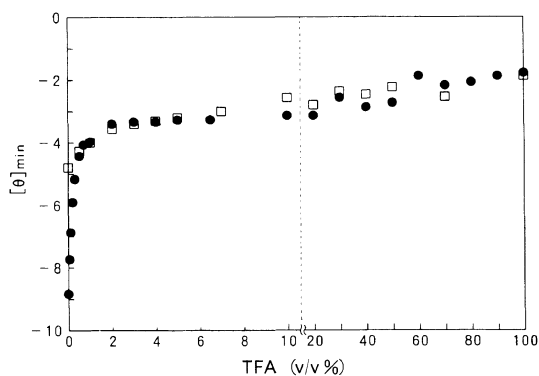


Figure 4. Dependence of TFA content on $[\theta]_{\min}$ for **II-H** (●), and **II-L** (□).

polypeptide **II-H**, $[\theta]_{\min}$ increased drastically in TFA content of 0—1.5 v/v% and moderately above 2.0 v/v%. In particular, at TFA content of 2—100 v/v%, $[\theta]_{\min}$ variation of polypeptide **II-H** was similar to that of polypeptide **II-L**. From a comparison of the two curves, we cannot conclude that the helical stability for polypeptide **II-H** is much higher than that for polypeptide **II-L**. Consequently, the increase of CD amplitudes with chain lengths should be ascribed not only to enhancement of helical stability, but also to helical interconversion induced by increasing chain length.

Estimation of Helical Type

Conformational energies and theoretical CD spectra were calculated to estimate the spatial arrangements of Δ^Z Phe residues or average helical main chains in the peptides $(X-\Delta^Z\text{Phe-Aib})_n$. Figure 5 shows the main-chain contour map. The conformational space was restricted severely to right- or left-handed helical regions, which correspond to the α - or 3_{10} -helix. Table I shows energy-minimized conformations listed from the lowest-energy to higher-energy ones. ΔE_{res} is the energy difference per residue from the lowest energy. All conformations with $\Delta E_{\text{res}} < 1.90 \text{ kcal mol}^{-1}$ showed the letter code AAA or A*A*A*, indicating that the polypeptide tends strongly to form common helices such as the α - and 3_{10} -helix. The results of

Figure 5 and Table I might reflect high helical stability indicated in the CD spectra in 100% TFA. The lowest-energy conformation was

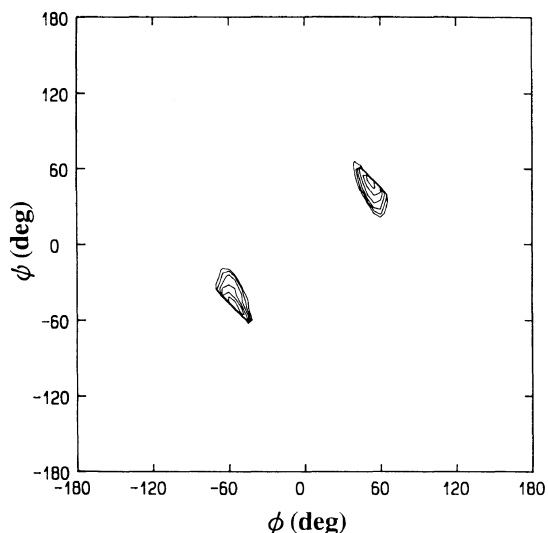


Figure 5. Main-chain energy contour map for Ac-(Ala- Δ^2 Phe-Aib) $_8$ -NMA. The contours are drawn in 0.5-kcal[mol(per residues)] $^{-1}$ increments from the energy minimum point (-56° , -48°).

found to be a right-handed helix (AAA), as shown in Figure 6. This conformation is stabilized by 3_{10} -helical-type and α -helical-type H-bonds, *i.e.*, (Aib $_i$)CO \leftarrow NH(Ala $_{i+3}$), (Aib $_i$)CO \leftarrow NH(Δ^2 Phe $_{i+4}$), and (Δ^2 Phe $_i$)CO \leftarrow NH(Aib $_{i+4}$), indicating that the polypeptide forms a right-handed 3_{10} - and/or α -helix. Here β -phenyl groups are helically arranged and the center-to-center distance between the nearest phenyl pairs is 6.1 Å. The second low-energy conformation was a left-handed helix, which is destabilized due to its relatively high energy ($\Delta E_{\text{res}} = 0.88$ kcal mol $^{-1}$).

Theoretical CD spectra were calculated on the basis of the spatial Δ^2 Phe arrangement for a given helix. The number (n) of repeating units (Ala- Δ^2 Phe-Aib) for polypeptide **II** was taken to be 8: CD spectrum divided by n was almost the same in $n \geq 8$. CD spectra calculated for the right-handed helical regions in Figure 5 showed exciton couplets with negative peaks at longer wavelengths, and those for the left-handed helical regions showed exciton

Table I. Energy-minimized conformations^a for Ac-(Ala- Δ^2 Phe-Aib) $_8$ -NMA

Conformational letter code	Ala		Δ^2 Phe			Aib		ΔE_{res}^b kcal mol $^{-1}$
	ϕ	ψ	ϕ	ψ	χ_2	ϕ	ψ	
AAA	-76	-41	-52	-34	139	-53	-47	0.00
A*A*A*	55	51	49	51	40	54	50	0.88
AAA	-70	-42	-54	-29	55	-53	-42	1.02
A*A*A*	54	55	46	52	119	54	49	1.33
FAA	-76	144	59	23	40	50	45	1.94

^aAll minima with $\Delta E_{\text{res}} < 2.0$ kcal mol $^{-1}$ are shown. ^b $E_0 = 108.9$ kcal mol $^{-1}$. $\Delta E_{\text{res}} = (E - E_0)/24$.

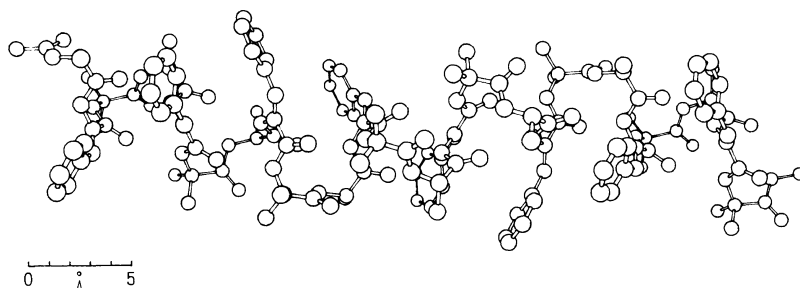


Figure 6. Lowest-energy conformation of Ac-(Ala- Δ^2 Phe-Aib) $_8$ -NMA in Table I.

couplets with the opposite sign. Thus, the experimental CD patterns indicate that the sequential peptides $(X-\Delta^2\text{Phe-Aib})_n$ are in right-handed helices. This is supported by the right-handed helix of the global minimum in Table I.

As described before, theoretical amplitudes of exciton couplets (A_t) depend on $\Delta^2\text{Phe}$ arrangements, particularly on the screw angle τ . Thus, the average $\Delta^2\text{Phe}$ arrangement or the average helical main chains can be predicted by searching the (ϕ, ψ) on which A_t agrees with the experimental amplitudes of exciton couplets (A_{exp}). For example, searching for polypeptide **II-H** in chloroform was carried out as follows. A_t for $\text{Ac}-(\text{Ala}-\Delta^2\text{Phe-Aib})_8-\text{NMA}$ was calculated fixing all ϕ to a given value (-70° , -65° , -60° , -55° , -50° , or -45°) and changing all ψ at 0.5° from -70° to

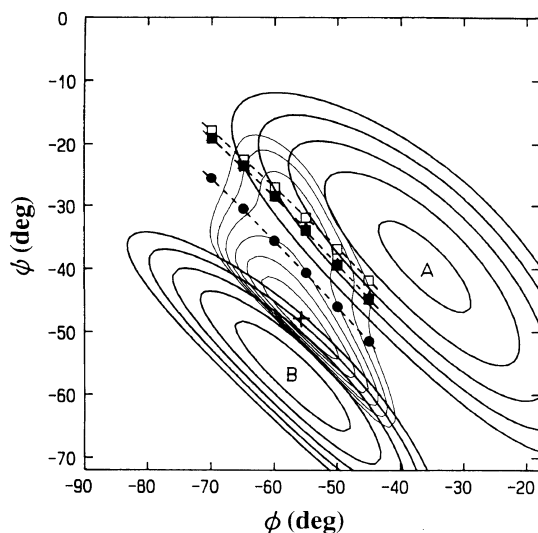


Figure 7(a). Expanded main-chain energy contour map represented by thin solid lines. The contours are drawn in $0.5\text{-kcal}[\text{mol}(\text{per residues})]^{-1}$ increments from the energy minimum point (+) of $(-56^\circ, -48^\circ)$. Bold solid contours represent (A) $\text{O}_i\leftarrow\text{H}_{i+3}(\text{N})$ (3_{10} -helical-type H-bonding) distance, and (B) $\text{O}_i\leftarrow\text{H}_{i+4}(\text{N})$ (α -helical-type H-bonding) distance. The contours are drawn in 0.1-\AA increments from 1.7 (the innermost contours) to 2.1 \AA . Dashed lines represent main chains to reproduce A_{exp} in chloroform for **II-H** (\bullet), **II-M** (\blacktriangle), **II-L** (\blacksquare), **I-4** (\circ), **I-3** (\triangle), and **I-2** (\square). The four plots of **II-M**, **II-L**, **I-4**, and **I-3** overlap each other.

0° . For each ϕ, ψ for which A_t is closest to A_{exp} ($=1.5 \times 10^5$) was sought.

(ϕ, ψ) pairs to reproduce A_{exp} for polypeptides and oligopeptides are plotted on the energy contour map for right-handed regions in Figure 7(a) (in chloroform) and in Figure 7(b) (in TMP). Contour lines of the $\text{O}_i\leftarrow\text{H}_{i+3}(\text{N})$ (3_{10} -helical-type H-bonding) and $\text{O}_i\leftarrow\text{H}_{i+4}(\text{N})$ (α -helical-type H-bonding) distances are superimposed on Figure 7. Here average $\text{O}\leftarrow\text{H}(\text{N})$ distances were calculated for all $\text{O}_i\leftarrow\text{H}_{i+3}(\text{N})$ and $\text{O}_i\leftarrow\text{H}_{i+4}(\text{N})$ pairs in $\text{Ac}-(\text{Ala}-\Delta^2\text{Phe-Aib})_8-\text{NMA}$, changing all ϕ and ψ at 1° . As a result, two kinds of H-bonding conformations, 3_{10} - and α -helices, were separated in distinct regions on (ϕ, ψ) space.

For oligopeptides **I-2** to **I-4** in chloroform or in TMP, three kinds of plots appeared close to each other. These main chains correspond to a right-handed helix with 3.2–3.3 residues

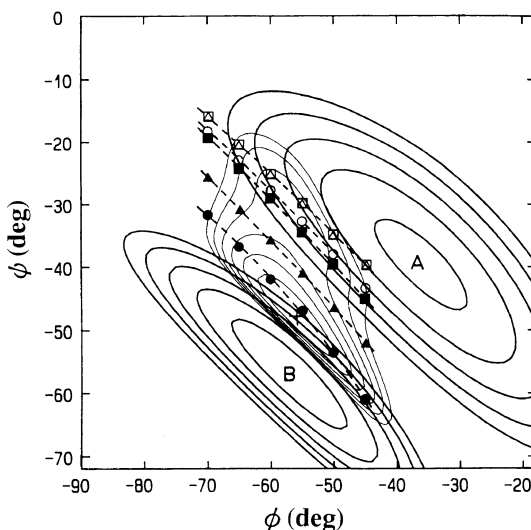


Figure 7(b). Expanded main-chain energy contour map represented by thin solid lines. The contours are drawn in $0.5\text{-kcal}[\text{mol}(\text{per residues})]^{-1}$ increments from the energy minimum point (+) of $(-56^\circ, -48^\circ)$. Bold solid contours represent (A) $\text{O}_i\leftarrow\text{H}_{i+3}(\text{N})$ (3_{10} -helical-type H-bonding) distance, and (B) $\text{O}_i\leftarrow\text{H}_{i+4}(\text{N})$ (α -helical-type H-bonding) distance. The contours are drawn in 0.1-\AA increments from 1.7 (the innermost contours) to 2.1 \AA . Dashed lines represent main chains to reproduce A_{exp} in TMP for **II-H** (\bullet), **II-M** (\blacktriangle), **II-L** (\blacksquare), **I-4** (\circ), **I-3** (\triangle), and **I-2** (\square).

per turn. (This helix should replace the “3.13₁₀-helix” reported in the previous study,¹⁸ because A_1 therein was erroneously represented as half the correct A_1 .) By superimposing their plots on the energy contour map, probable conformations for peptides **I-2** to **I-4** should fall on an area around (-55° , -33°). These helical conformations are in a 3₁₀-helical-type H-bonding region.

In common CD calculations including the above CD calculation, all irregularities and thermal fluctuations of a given conformation are usually excluded, although such factors should reduce CD amplitudes calculated for the fixed conformation. In fact, helical polypeptides containing arylalanines show smaller experimental CD amplitudes relative to the theoretical ones calculated for fixed conformations.²⁷⁻²⁹ This is mainly considered to be due to thermal fluctuation in the polypeptides. Thus, the actual helices of (poly)peptides **I-n** and **II** may comprise not only the helices estimated here, but other types of helices that shows larger A_1 . Namely, A_1 in Figure 7, speaking roughly, increases with helical type changing from 3.2–3.3 residues to more residues per turn, *i.e.*, from 3₁₀-helical-type to α -helical-type H-bonding regions. Accordingly, actual helices may range from a 3₁₀-helix around (-55° , -33°) up to an α -helix.

The ¹H NMR study¹⁸ indicated that peptides **I-2** to **I-4** in CDCl₃ have a 3₁₀-helical H-bonding pattern, but not α -helical pattern. Therefore, average main-chain conformations for oligopeptides **I-2** to **I-4** should be in a helix with a 3₁₀-type helix with 3.2–3.3 residues per turn.

For polypeptides **II-L** and **II-M** in chloroform, (ϕ , ψ) plots to reproduce the A_{exp} appeared at regions similar to those for the oligopeptides. Thus, the two polypeptides in chloroform also form a right-handed helix with 3.2–3.3 residues per turn, similarly to oligopeptides **I-2** to **I-4**. The plot for polypeptide **II-H** in chloroform deviated from those for polypeptides **II-L** and **II-M**. This direction of

deviation is from 3₁₀- to α -helical regions. It was observed more prominently in TMP that the helical type changes with increasing chain length, as in Figure 7(b). Namely, helix interconversion in peptides (X- Δ^Z Phe-Aib)_{*n*} is induced by increasing chain length.

Helix interconversion has been found in Aib-containing peptides^{36,37}: *e.g.*, in peptides *p*-bromobenzoyl-(Aib-Ala)_{*m*}-OMe. The hexapeptide (*m*=3) is in a complete 3₁₀-helix, but the decapeptide (*m*=5) and dodecapeptide (*m*=6) are in an α -helix. On the other hand, interconversion in peptides (X- Δ^Z Phe-Aib)_{*n*} occurs at least at chain lengths above the dodecapeptide (*n*=4). According to a modified Zimm–Bragg-type model,³⁸ the chain length to induce the 3₁₀/ α -helical transitions increases with peptide composition of Aib residues that favor the 3₁₀-helical conformation. Δ^Z Phe residues also tend to form 3₁₀-helical-type bonds as observed in several Δ^Z Phe-containing oligopeptides.⁶⁻¹³ Consequently, that the transition length for (X- Δ^Z Phe-Aib)_{*n*} is longer than that for (Aib-Ala)_{*m*} may be related to increase in 3₁₀-helical-type H-bonding residues (Aib and Δ^Z Phe).

However, we cannot determine whether the helix interconversion in question occurs drastically at certain chain lengths or gradually with increasing chain length, because the studied polypeptides have polydispersity in MWs, and MWs are not absolute. Further, the equilibrium between 3₁₀- and α -helices or presence of 3₁₀/ α -helix mixtures cannot be denied. At least, we claim that polypeptide **II** changes its average helix type (Δ^Z Phe spatial arrangement) with increasing chain length. To clarify helix interconversion in Δ^Z Phe-containing peptides, our current efforts are directed toward conformational analysis of other sequential oligopeptides without Aib residues.

CONCLUSIONS

We synthesized the sequential polypeptide, poly[Lys(Z)- Δ^Z Phe-Aib], to design peptides

containing helically-arranged Δ^2 Phe side chains, and investigated its solution conformation based on CD analysis and conformational energy calculation. Experimentally and theoretically, this polypeptide was found to form a highly stable right-handed 3_{10} - or α -type helix. Here β -phenyl groups tightly-bound to the backbone are arranged regularly along the helical axis. This will be useful for designing a highly stable helical backbone on which β -substituents of dehydro residues are regularly arranged.

Acknowledgment. We express our sincere gratitude to Professor M. Kawai in Department of Applied Chemistry, Nagoya Institute of Technology for recording CD spectra.

REFERENCES

1. K. Noda, Y. Shimohigashi, and N. Izumiya, "The Peptides," Vol 5, E. Gross and J. Meienhofer, Ed., Academic Press, New York, N.Y., 1983, pp 286—339.
2. E. Gross and J. L. Morell, *J. Am. Chem. Soc.*, **89**, 2791 (1967).
3. H. Allgaier, G. Jung, R. G. Werner, U. Schneider, and H. Zaehner, *Eur. J. Biochem.*, **160**, 9 (1986).
4. I. L. Givot, T. A. Smit, and R. H. Abeles, *J. Biol. Chem.*, **244**, 6341 (1969).
5. R. B. Wickner, *J. Biol. Chem.*, **244**, 6550 (1969).
6. K. Uma and P. Balaram, *Indian J. Chem.*, **28B**, 705 (1989), and references therein.
7. K. R. Rajashankar, S. Ramakumar, and V. S. Chauhan, *J. Am. Chem. Soc.*, **114**, 9225 (1992).
8. O. Pieroni, A. Fissi, C. Pratesi, P. A. Temussi, and F. Ciardelli, *J. Am. Chem. Soc.*, **113**, 6338 (1991).
9. M. R. Ciajolo, A. Tuzi, C. R. Pratesi, and A. Fissi, and O. Pieroni, *Biopolymers*, **30**, 911 (1990).
10. K. K. Bhandary and V. S. Chauhan, *Biopolymers*, **33**, 209 (1993).
11. B. Padmanbhan and T. P. Singh, *Biopolymers*, **33**, 613 (1993).
12. V. S. Chauhan, K. Uma, P. Kaur, and P. Balaram, *Biopolymers*, **28**, 763 (1989).
13. M. R. Ciajoro, A. Tuzi, C. R. Pratesi, A. Fissi, and O. Pieroni, *Biopolymers*, **32**, 717 (1992).
14. A. Gupta, A. Bharadwaj, and V. S. Chauhan, *J. Chem. Soc., Perkin Trans. 2*, 1911 (1990).
15. L. Piela, G. Nemethy, and H. A. Scheraga, *Biopolymers*, **26**, 1273 (1987).
16. M. Vásquez, G. Nemethy, and H. A. Scheraga, *Macromolecules*, **10**, 1 (1983).
17. S. S. Zimmerman, M. S. Pottle, G. Nemethy, and H. A. Scheraga, *Macromolecules*, **16**, 1043 (1977).
18. Y. Inai, T. Ito, T. Hirabayashi, and K. Yokota, *Biopolymers*, **33**, 1173 (1993).
19. N. Nishi, T. Naruse, K. Hagiwara, B. Nakajima, and S. Tokura, *Makromol. Chem.*, **192**, 1799 (1991).
20. F. Momany, R. F. McGuire, A. W. Burgess, and H. A. Scheraga, *J. Phys. Chem.*, **79**, 2361 (1975).
21. D. Ajō, G. Granozzi, and E. Tondello, *J. Mol. Struct.*, **41**, 131 (1977).
22. D. Ajō, A. D. Prā, and G. Zanotti, *J. Chem. Soc., Perkin Trans. 2*, 927 (1979).
23. D. Ajō, M. Casarin, and G. Granozzi, *J. Mol. Struct.*, **86**, 420 (1982).
24. M. Sisido, private communications.
25. Y. Beppu, *Comput. Chem.*, **13**, 101 (1989).
26. D. Ajō, V. Buseti, and G. Granozzi, *Tetrahedron*, **38**, 3329 (1982).
27. M. Sisido and Y. Imanishi, *Macromolecules*, **19**, 2187 (1986).
28. M. Sisido, *Macromolecules*, **22**, 3280 (1989).
29. M. Sisido, *Macromolecules*, **22**, 4367 (1989).
30. M. Oka, Y. Baba, A. Kagemoto, and A. Nakajima, *Polym. J.*, **26**, 135 (1990).
31. M. Oka and A. Nakajima, *Polym. Bull.*, **30**, 647 (1993).
32. S. S. Zimmerman, M. S. Pottle, G. Nemethy, and H. A. Scheraga, *Macromolecules*, **10**, 1 (1977).
33. N. Harada, S. L. Chen, and K. Nakanishi, *J. Am. Chem. Soc.*, **97**, 5345 (1975).
34. O. Pieroni, G. Montagnoli, A. Fissi, S. Merlino, and F. Ciardelli, *J. Am. Chem. Soc.*, **97**, 6820 (1975).
35. S. Egusa, M. Sisido, and Y. Imanishi, *Polym. J.*, **18**, 403 (1986).
36. E. Benedetti, D. B. Benedetto, V. Pavone, C. Pedone, A. Santini, A. Bavoso, C. Toniolo, M. Crisma, and L. Sartore, *J. Chem. Soc., Perkin Trans. 2*, 1829 (1990).
37. V. Pavone, E. Benedetti, B. DiBlasio, C. Pedone, A. Santini, A. Bavoso, C. Toniolo, M. Crisma, and L. Sartore, *J. Biomol. Struct. Dynam.*, **7**, 1321 (1990).
38. G. Basu and A. Kuki, *Biopolymers*, **32**, 61 (1992).